International Journal of Automation and Computing
www.ijac.net

18(6), December 2021, 993-1006
DOI: 10.1007/s11633-021-1305-0

A Signal Based "W" Structural Elements for Multi-scale Mathematical Morphology Analysis and Application to Fault Diagnosis of Rolling Bearings of Wind Turbines

Qiang Li[1,2] Yong-Sheng Qi[1,2] Xue-Jin Gao[3] Yong-Ting Li[1,2] Li-Qiang Liu[1,2]

[1] Institute of Electric Power, Inner Mongolia University of Technology, Hohhot 010080, China

[2] Inner Mongolia Key Laboratory of Electrical and Mechanical Control, Hohhot 010051, China

[3] Faculty of Information, Beijing University of Technology, Beijing 100124, China

Abstract: Working conditions of rolling bearings of wind turbine generators are complicated, and their vibration signals often show non-linear and non-stationary characteristics. In order to improve the efficiency of feature extraction of wind turbine rolling bearings and to strengthen the feature information, a new structural element and an adaptive algorithm based on the peak energy are proposed, which are combined with spectral correlation analysis to form a fault diagnosis algorithm for wind turbine rolling bearings. The proposed method firstly addresses the problem of impulsive signal omissions that are prone to occur in the process of fault feature extraction of traditional structural elements and proposes a "W" structural element to capture more characteristic information. Then, the proposed method selects the scale of multi-scale mathematical morphology, aiming at the problem of multi-scale mathematical morphology scale selection and structural element expansion law. An adaptive algorithm based on peak energy is proposed to carry out morphological scale selection and structural element expansion by improving the computing efficiency and enhancing the feature extraction effect. Finally, the proposed method performs spectral correlation analysis in the frequency domain for an unknown signal of the extracted feature and identifies the fault based on the correlation coefficient. The method is verified by numerical examples using experimental rig bearing data and actual wind field acquisition data and compared with traditional triangular and flat structural elements. The experimental results show that the new structural elements can more effectively extract the pulses in the signal and reduce noise interference, and the fault-diagnosis algorithm can accurately identify the fault category and improve the reliability of the results.

Keywords: Fault diagnosis, structural element, multi-scale mathematical morphology, rolling bearing, correlation analysis.

Citation: Q. Li, Y. S. Qi, X. J. Gao, Y. T. Li, L. Q. Liu. A signal based "W" structural elements for multi-scale mathematical morphology analysis and application to fault diagnosis of rolling bearings of wind turbines. *International Journal of Automation and Computing*, vol.18, no.6, pp.993–1006, 2021. http://doi.org/10.1007/s11633-021-1305-0

1 Introduction

Rolling bearing is one of the most commonly used and most vulnerable main components in the chain drive system of wind turbines. This failure can cause costly production losses and lead to catastrophic accidents. Therefore, early detection[1], diagnosis[2, 3], and prediction of remaining useful life[4] of the defects in rolling bearings during the operation of wind turbines are conducive to avoid abnormal events and reduce production losses. At present, the analysis of vibration signals is one of the most commonly used methods for diagnosing rolling bearings. It is of great significance to improve the accuracy of fault diagnosis results by extracting fault features accurately and efficiently from non-stationary and non-linear vibration signals.

Mathematical morphological analysis[5] is a non-linear signal processing method developed in recent years, which can decompose a vibration signal into several components by retaining the morphological characteristics of the signal according to the geometric characteristics of the structural elements. At present, many researchers are attempting to extract relevant fault features from vibration signals through mathematical morphology for identifying the root cause of the fault more effectively. Nikolaou and Antoniadis[6] introduced single-scale mathematical morphology in the fault diagnosis of rolling bearings, where the scale refers to the height and length of the structural elements (SE). Before using the single-scale mathematical morphology, the structural element must be determined first. The height and length remain unchanged during the subsequent morphological processing. Mao et al.[7] utilized a feature extraction technique with

Research Article
Manuscript received February 1, 2021; accepted April 29, 2021; published online June 1, 2021
Recommended by Associate Editor Jie Zhang
Colored figures are available in the online version at https://link.springer.com/journal/11633

generalized fractal dimension based on mathematical morphology. Then, they extracted the characteristic combustion signal for monitoring the combustion state. Shen et al.[8] proposed a signal processing method based on a generalized mathematical morphological filter for eliminating non-linear noise in vibration signals. This method shows that morphological filtering has obvious effects in suppressing signal noise and extracting impulse components of the original signals. However, since the length and height of the single-scale mathematical morphology structural elements are set as fixed values, the feature information extracted from the original signal by a single-scale mathematical morphology is very limited.

In order to extract more characteristic information from vibration signals, Maragos[9] proposed a multi-scale mathematical morphology method. In this method, the single-scale structural elements are transformed into a series of structural elements based on certain rules. Moreover, the characteristic information at different scales is extracted and further processed to form the morphological spectrum. Li et al.[10] proposed a fault diagnosis method that uses multi-scale morphological analysis for extracting impulse features from strong background noise signals. Cui et al.[11] proposed a multi-scale morphological filtering algorithm for early faults of rolling bearings based on information entropy threshold (IET-MMF) to extract fault features in vibration signals. Zhang[12] surveyed the application of multi-scale mathematical morphology in vibration signal processing. Wu et al.[13] used a noise-assisted multivariate empirical mode decomposition combined with a multi-scale morphology method of bearing fault diagnosis. All the above methods show that multi-scale mathematical morphology has an obvious advantage over single-scale in feature extraction. This advantage is mainly manifested in the analysis of the multi-scale mathematical morphology through structural elements of various scales. It can maintain the pulse details at small scales and effectively suppress a large-scale noise. However, there is no unified standard for scale selection and structure element construction in multi-scale morphological operation. Li et al.[14] used multi-scale mathematical morphology to extract the features of rolling bearings. In order to ensure the effect of feature extraction, the operation scale may be large, and the width of the flat structure elements increases with the scale. Although the fault frequency of the outer and inner of the rolling bearing can be extracted, the operation is complicated.

A structural element is an important part of multi-scale mathematical morphology, and its structural characteristics have a vital influence on the analysis of results of mathematical morphology. It is an array of certain geometric characteristics composed of a series of discrete data. A structural element is determined in terms of shape, height (size of element), and length (number of elements)[15]. The most common structural elements are flat, triangular, and sinusoidal. Among them, the flat and triangular types are the most used structural elements when vibration signals of a bearing are analyzed and processed[16, 17]. However, since there are a large number of sudden changes in the fault signals of rolling bearings and these two structural elements do not contain sudden pulse changes, the feature extraction effect of the bearing fault signals is often not ideal, and it may easily miss the pulse fault signal.

Considering the above problems, this paper aims to capture numbers of sudden changes in the rolling bearing fault signal by starting from the detailed characteristics of a signal. Accordingly, a more suitable "W" structural element is proposed for fault vibration signal analysis. This new structural element not only conforms to the structural characteristics of the vibration signal in the center part but also at both ends. The addition of two abrupt components can solve the problem of missing abrupt pulse signals by flat and triangular structural elements. Furthermore, to solve the problems of scale selection in multi-scale mathematical morphology operations and the construction of multi-scale structural elements, this paper proposes an adaptive multi-scale construction method based on peak energy. In this method, the separation distance between peaks is used to determine the morphological scale.

Moreover, the change of peak energy is utilized to determine the range of change in the height of structural elements. Hence, selecting scales is solved in multi-scale mathematical morphological operations, and the multi-scale structure is optimized. This technique reduces computational complexity and enhances computational efficiency while ensuring the effect of feature extraction. Finally, in numerical examples, bearing platform data obtained from Western Reserve University and real wind turbine data are used to validate the algorithm and compared with traditional flat and triangular structural elements.

The rest of the paper is organized as follows. The basic knowledge is described in Section 2. New structural elements and multi-scale construction methods are introduced in Section 3, followed by the fault diagnosis algorithm in Section 4. Finally, the paper is concluded in Section 5.

2 Basic knowledge

2.1 Mathematical morphology

Mathematical morphology is an effective tool for signal processing in the time domain. It uses structural elements with certain geometric characteristics to locally match or modify a signal to extract and denoise signal features.

Mathematical morphology has four basic operations, namely corrosion, expansion, opening operation, and closing operation. The operation formulas are as follows:

Let $f(n)$ denote a one-dimensional discrete signal, and the structural element $g(m)$ denote the discrete sequence defined as $G = (0, 1, \cdots, M-1)$. Then, the corrosion and expansion operations can be expressed by (1) and (2), respectively.

$$(f \Theta g)(n) = \min\left[f(n+m) - g(m)\right] \tag{1}$$

$$(f \oplus g)(n) = \max\left[f(n-m) + g(m)\right]. \tag{2}$$

In (1) and (2), $m \in 0, 1, \cdots, M-1$, Θ represents the corrosion operator, and $\oplus$ represents the expansion operator.

Based on the corrosion and expansion operations, the morphological opening and closing operations can be expressed by (3) and (4), respectively.

$$(f \circ g)(n) = (f \Theta g \oplus g)(n) \tag{3}$$

$$(f \cdot g)(n) = (f \oplus g \Theta g)(n). \tag{4}$$

In (3) and (4), $\circ$ represents the open operator, and $\cdot$ represents the closed operator.

2.2 Multi-scale mathematical morphology and morphological spectrum

On the basis of single-scale mathematical morphology, a new variable scale λ is introduced here, through which a sequence of structural elements of different scales is generated for performing multi-scale and multi-level analysis of the signal to be processed. For this purpose, the following opening and closing operations are defined in multi-scale morphology.

$$(f \circ g)_\lambda = (f \Theta \lambda g) \oplus \lambda g = f \circ \lambda g \tag{5}$$

$$(f \cdot g)_\lambda = (f \oplus \lambda g) \Theta \lambda g = f \cdot \lambda g. \tag{6}$$

The above (5) and (6) represent the multi-scale opening and closing operations of the structural element g at the scale λ (1, 2, 3, ⋯).

Morphological spectrum, also known as the histogram of shape value, is a quantitative description of shape representation in signal analysis. The morphological spectrum combines the results of multi-scale morphological operations. The multi-scale morphological spectrum of the original signal f relative to the structural element g is defined as

$$\begin{aligned} PS_+(+\lambda, g) &= A\left[f \circ \lambda g - f \circ (\lambda+1)\, g\right] \\ PS_-(-\lambda, g) &= A\left[f \cdot \lambda g - f \cdot (\lambda-1)\, g\right] \\ A(f) &= \sum_n f(n). \end{aligned} \tag{7}$$

In (7) and (8), λ represents the scale of the structural element.

2.3 Structural element

Structural elements are the basic operators of mathematical morphology operations. The extraction of vibration signal features is affected by structural elements and mathematical morphology operations. Structural element function is similar to that of a feature extraction "window". The more similar the geometric features of the selected "window" to the signal framed by the "window", the more the feature information that can be extracted from this part of the signal. Common structural elements are flat, triangular, and sinusoidal, which are shown in Fig. 1.

2.4 Correlation analysis

The correlation analysis is a classification tool that measures the similarity of two sets of data of the same size. At present, correlation analysis has been widely used in the field of signal processing[17, 18].

In order to measure the degree of correlation between two columns of data, a correlation coefficient is defined in (8).

$$r = \frac{Cov(x(t), y(t))}{\sigma_x \sigma_y} \tag{8}$$

where r is the correlation coefficient, $x(t)$ is the training signal, $y(t)$ is the signal to be measured, σ_x and σ_y are the standard deviations of $x(t)$ and $y(t)$.

3 New structural elements and multi-scale construction methods

3.1 "W" structural element

Traditional research on mathematical morphology is

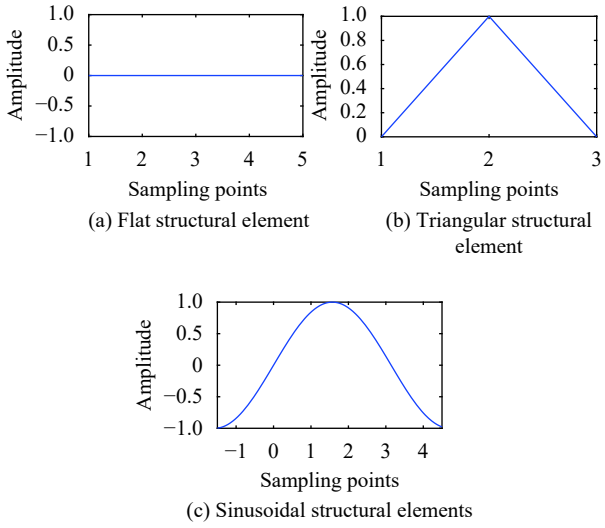

Fig. 1 Several common structural elements

based on the characteristics of the signal used to select structural elements for achieving better processing results. However, since the vibration signals collected under actual working conditions are often complex, the noise is usually not unique. The traditional structural elements have no satisfactory performance to analyze and process the signal.

Fig. 2 shows the time domain diagram of the fault signal of the inner ring of a bearing having a damage diameter of 0.007. It can be seen that the waveform of the vibration signal conforms to the zero-axis symmetry and exhibits non-linear characteristics. There are triangular-like spikes in the signal. At the same time, there are mutation signals of different sizes at both ends. However, traditional structural elements often consider only the impulse response in the vibration signal and ignore the abrupt components on both sides, which leads to the omission of some signal characteristics. Therefore, structural elements are required to be sensitive to impulse responses and sudden changes in the signal so as to ensure effectiveness in feature extraction.

To overcome the problems of structural elements, this paper proposes a novel structural element to simultaneously capture the impulse response appearing in the signal and the abrupt signal and meet the extraction requirements of complex signal features. The structure of the proposed element is shown in Fig. 3. A spike-like pulse of a vibration signal is resembled by the central part of the new structural element. Moreover, a non-zero element is added to both ends. Since the shape is similar to the letter "W", we named this structural element as the "W"-shaped structural element. So far, based on the center height of the structural element, we define a matrix form of the structural element as $[h \ \ 0 \ \ h \ \ 0 \ \ h]$.

The "W" and triangular structural elements are subjected to fast Fourier transform. In order to better explain the meaning of the "W" structural element, a comparative analysis is carried out from the perspective of the frequency domain. Fig. 4 (a) shows the frequency spectrum of the triangular structural element, whose matrix form is [0 0.5 1 0.5 0], and the number of sampling points is $N = 128$. As seen in Fig. 4 (a) the spectrum diagram of the triangular structure elements is similar to the amplitude-frequency characteristics of the low-pass filter. This can smooth high-frequency and abrupt parts of the signal. Moreover, the fault and noise in the vibration signal are often high-frequency mutations and easy to be filtered out. The signal often appears in the high-frequency part. Although triangular structural can play a certain filtering role, it ignores the important fault information. Fig. 4 (b) shows the frequency spectrum of the "W" structural element, whose matrix form is [1 0 1 0 1], and the number of sampling points is $N = 128$. It can be seen in Fig. 4 (b) that there is a clear difference between the frequency spectrum and the triangular structural element.

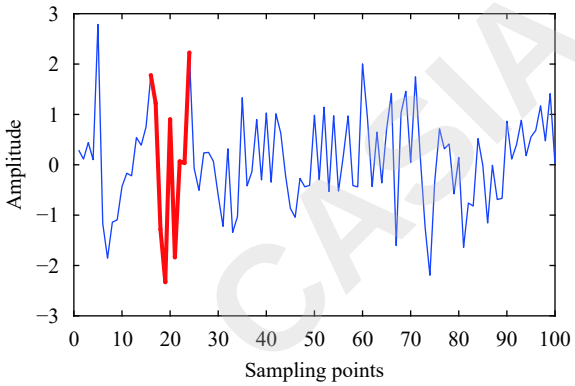

Fig. 2 Time domain diagram of fault signal of the inner ring of a bearing having damage diameter of 0.007

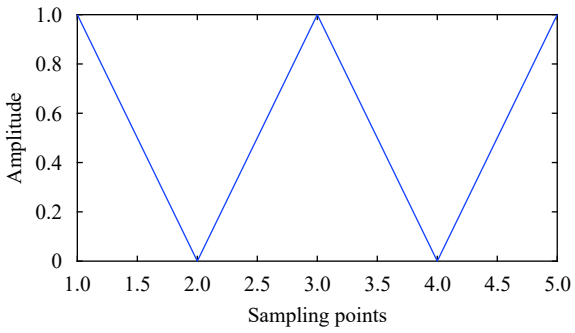

Fig. 3 "W" structural elements

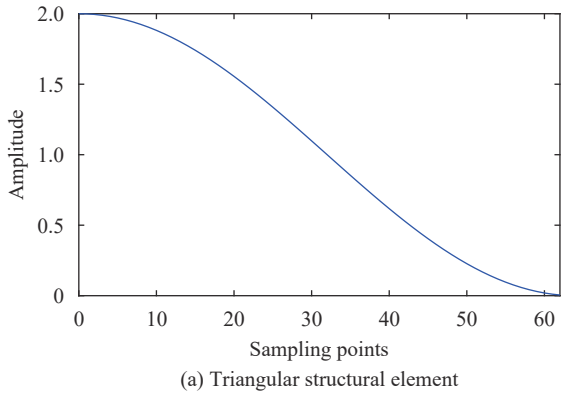

(a) Triangular structural element

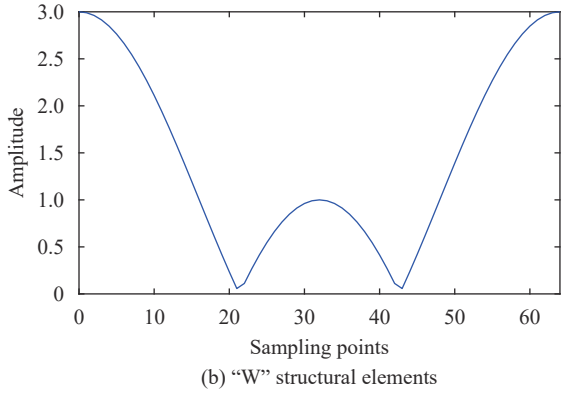

(b) "W" structural elements

Fig. 4 Amplitude-frequency diagram of two structural elements

Based on Fig. 4, the spectrum of the "W" structural element is obviously different from that of the triangular structural element. Both ends and the central part of the "W" structural element allow the passage of high-frequency signals. Hence, the abrupt signal can be greatly retained in the signal, which is more appropriate for the analysis of complex vibration signals.

3.2 Adaptive algorithm based on peak energy

In the traditional multi-scale mathematical morphology operation, a series of structural elements are produced by determining scale λ, which greatly influences the feature extraction of vibration signals according to the scale. However, there is no standard selection principle for the above issues. Hence, it is difficult to achieve the best feature extraction performance.

In order to tackle the above problems, this paper takes the peak of the signal as the starting point and adapts the morphological scale for determining the sequence of structural elements. Firstly, the morphological scale λ is determined using the maximum spacing distance between adjacent peaks in the signal. Then, the peak energy of the signal and the maximum difference of the peak energy are calculated. Finally, the scale and energy differences are used to optimize the multi-scale structural elements. This method can cover the peak information in the signal, reduce unnecessary operation, and improve the efficiency of the operation.

Fig. 5 (a) shows some details of the collected actual vibration signal, where it can be found that the noise pollution is severe and the peak information is considerable. The peak value involved in the selection inevitably increases, the peak interval point becomes smaller, and the peak difference increases, resulting in a larger morphological scale selected. The variation range of the structural elements will increase, thereby the effect of mathematical morphological feature extraction will be weakened. Therefore, before determining the morphological scale and the sequence of structural elements, this article first obtains the peak energy of the signal, whose variance is used as the threshold limit as shown by the dotted line in Fig. 5 (b). In order to reduce noise interference, the excess noise peaks are eliminated from the signal as much as possible by screening and retaining the peak points greater than the threshold.

According to the above analysis, this paper proposes an adaptive algorithm based on peak energy. In this algorithm, the variance of the peak energy is used as the threshold limit, the peak information is filtered, the morphological scale is calculated, and the sequence of structural elements is determined according to λ. The reason for such choice is as follows: In general, the amplitude of the noise component is smaller than the fault pulse. By calculating the peak energy, the pulse component with a smaller amplitude can be made smaller, and the pulse component with a large amplitude can be amplified at the same time. The separation of a noise signal and a fault signal is made easier. Then the peak energy of the signal is calculated as the threshold limit so that the threshold limit can be distinguished from noise and fault pulse. In this way, the peak points larger than the threshold line are the fault pulse points. Ultimately, the height variation range of structural elements is determined based on the maximum difference of peak energy. The adaptive algorithm based on the peak energy can be summarized in the following steps:

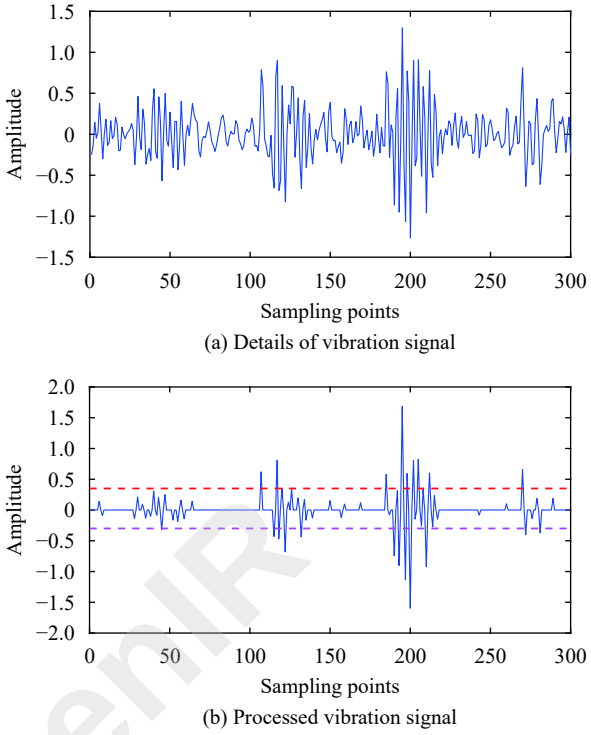

Fig. 5 Vibration signal

1) Firstly, perform zero-average processing on the vibration signal $f(n)$ to obtain $y(n) = \{y_n | n = 1, 2, \cdots, N\}$.

2) Search for all positive peak points $Q = \{q_i | i = 1, 2, \cdots, I\}$ in signal $y(n)$, calculate the energy of the peak points according to $M = kQ^2$, and take $k = 1$ in this article. Then, find the variance m of the peak energy, and divide the known positive peak points according to m as the threshold, keep the positive peak points larger than m, and eliminate the positive peak points smaller than m. Generate a new set of the positive peak points $Q' = \{q'_j | j = 1, 2, \cdots, J\}$, where J represents the number of positive peak points whose amplitude is greater than m.

3) Calculate the number of interval sampling points between two adjacent peaks, determine the maximum interval sampling point number $L_{\max}$ and the minimum interval sampling point number $L_{\min}$, and set the initial length of the structural element as L_0. First, judge the size of $L_{\min}$ and L_0. If $L_0 > L_{\min}$, then let $L_{\min} = L_0$. At

this point, the scale $\lambda = L_{\min} - L_0 = 0$. If $L_0 < L_{\min}$, then let $L_{\min} = L_0$. At this point, the scale $\lambda = L_{\min} - L_0$. When the length of the structural element changes to $L_{\max}$, then the scale $\lambda = L_{\max} - L_0$ reaches the maximum. Therefore, the range of scale transformation of multi-scale mathematical morphology is

$$\lambda = \left\{ \begin{array}{l} L_{\min} - L_0, L_{\min} - L_0 + 1, \cdots, \\ L_{\max} - L_0 - 1, L_{\max} - L_0 \end{array} \right\}.$$

4) Search for the maximum, and minimum peak energy denoted as $M_{\max}$ and $M_{\min}$, respectively. Divide the maximum difference of peak energy $(M_{\max} - M_{\min})$ by the scale to calculate the degree of growth at each scale. Then, the height of the center point can be obtained as

$$h = \sqrt{M_{\min} + (M_{\max} - M_{\min}) / (L_{\max} - L_{\min})}$$

where $\lambda = 0, 1, 2, \cdots, L_{\max} - L_{\min}$.

5) Take the "W" structural element as an example. Suppose that the initial structural element matrix is

$$\mathrm{B} = \frac{h}{\lambda} [\lambda \quad A_1 \quad \lambda \quad A_2 \quad \lambda]$$

$$\mathrm{A}_1 = [1, 1, \cdots, 1]_{1\times\lambda} \begin{bmatrix} 0 & & & \\ & 1 & & \\ & & \cdots & \\ & & & \lambda \end{bmatrix}_{\lambda\times\lambda} =$$

$$e_\lambda^\tau \mathrm{diag}(0, 1, \cdots, \lambda - 1)$$

$$\mathrm{A}_2 = [1, 1, \cdots, 1]_{1\times\lambda} \begin{bmatrix} \lambda & & & \\ & \lambda - 1 & & \\ & & \cdots & \\ & & & 0 \end{bmatrix}_{\lambda\times\lambda} =$$

$$e_\lambda^\tau \mathrm{diag}(\lambda, \lambda - 1, \cdots, 0)$$

$$\lambda = \left\{ \begin{array}{l} L_{\min} - L_0, L_{\min} - L_0 + 1, \cdots, \\ L_{\max} - L_0 - 1, L_{\max} - L_0 \end{array} \right\}$$

where λ is the scale of mathematical morphology.

Through the above method, the scale $\lambda = L_{\max} - L_{\min}$ of multi-scale mathematical morphology is determined, and the multi-scale structural elements are constructed as shown in Fig. 6.

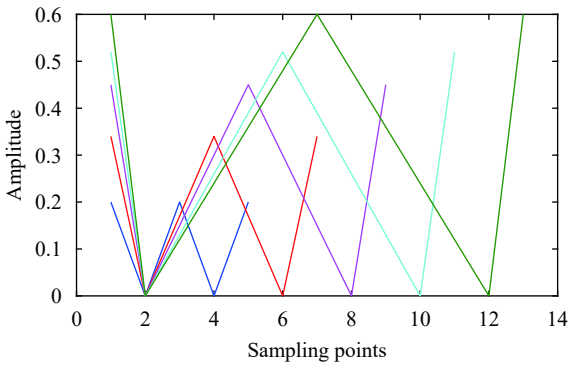

Fig. 6 Multi-scale "W" structural elements

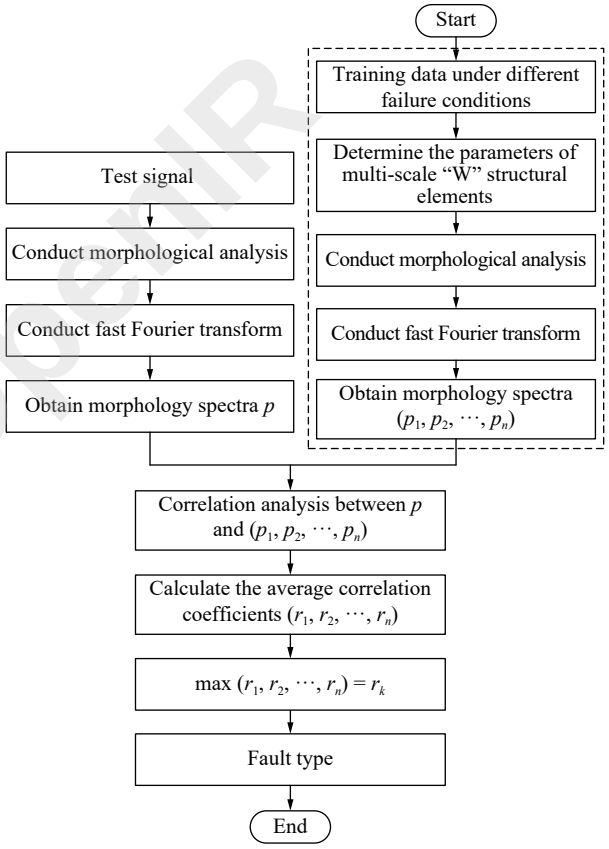

Fig. 7 Flow chart of fault diagnosis algorithm

4 Rolling bearing fault diagnosis algorithm based on multi-scale mathematical morphology of "W" structural element

4.1 Fault diagnosis algorithm

The flow chart of the diagnostic algorithm is shown in Fig. 7. The algorithm consists of two parts. The right half is the signal training module, training and extracting data from known normal, inner faults, and outer faults. The left half is the algorithm, which is applied to identify and diagnose the faults of the signal under test. The working steps of the algorithm are as follows:

1) According to the known types of faults, the training signals are divided into m categories. Each category contains n training sample signals. The obtained signal set is $\{x_{i,j}\}(i = 1, 2, \cdots, m; j = 1, 2, \cdots, n)$.

2) Perform multi-scale mathematical morphology operations on the signal set to extract the characteristic information of the signal $\{x_{i,j}\}$. Among them, "W" structural elements are selected, and adaptive algorithms based on the peak energy are used to determine the scale λ of multi-scale mathematical morphology and construct

multi-scale structural elements $SE_i\,(i=1,2,\cdots,\lambda)$.

3) The fast Fourier transform is used to transform the processed signal set $\{x_{i,j}\}(i=1,2,\cdots,m;j=1,2,\cdots n)$ and use (7) to obtain the corresponding morphological spectrum set $\{P_i\}\,(i=1,2,\cdots,m)$.

4) For bearing signals with unknown fault types, repeat Steps 2) and 3), perform multi-scale mathematical morphology operations, find the normalized morphological spectrum, and obtain the morphological spectrum P of the unknown signal.

5) Calculate the average correlation coefficient between the morphological spectrum P of the unknown signal and the trained adaptive morphological spectrum set $\{P_i\}\,(i=1,2,\cdots,m)$. Assuming that the largest one out of r_1 to r_m is $r_s\,(0<s<m)$, it is considered that the working state of the bearing corresponding to the unknown signal is the same as that corresponding to the training preprocessing signal set $\{x_i\}$, i.e., it is checked whether the unknown signal has a fault and the fault type to achieve the purpose of diagnosis.

4.2 Numerical example simulation

In order to verify the feature extraction effect of the multi-scale "W" structural element, a mixed-signal is constructed as (9):

$$y(t)=x_1(t)+x_2(t)+x_3(t) \tag{9}$$

where $x_1\,(t)=0.5\sin\,(2\pi\times 20t)+0.5\cos\,(2\pi\times 60t)$ represents repetitive shock response with a sinusoidal frequency of 20 Hz and cosine frequency of 60 Hz, $x_2\,(t)=0.05\mathrm{e}^{-t}\times\sin\,(2\pi\times 40t)$ represents an amplitude-modulated sinusoidal signal with a frequency of 40 Hz and exponentially attenuating, and $x_3\,(t)$ is defined as a Gaussian white noise with a mean value of 0 and a standard deviation of 1 which simulates mechanical background noise. Suppose the sampling frequency of the signal is 8 000 Hz, and the number of sampling points is 2 000. The corresponding time domain diagrams of the mixed-signal are shown in Figs. 8 (a) and 8 (b). In Figs. 8 (a) and 8 (b), the signal components with frequencies of 20 Hz and 60 Hz are clearly seen. The pulse signal with a frequency of 40 Hz is almost submerged in the noise signal. The open operation of mathematical morphology is performed on the mixed signals with "W", triangular and flat structural elements, and then the processed frequency domain images are compared. The frequency domain maps of the mixed signal filtered by the "W"-shaped, triangular and flat structural elements are shown in Figs. 8 (c)–8 (e), respectively. The comparative analysis shows that the "W" structural element has a better noise reduction effect than the triangular and flat structural elements. The extraction effect of the 40 Hz pulse signal submerged in the noise signal is more obvious. To a certain extent, it shows that the "W"-shaped structural elements can extract the pulse components submerged in the signal more effectively.

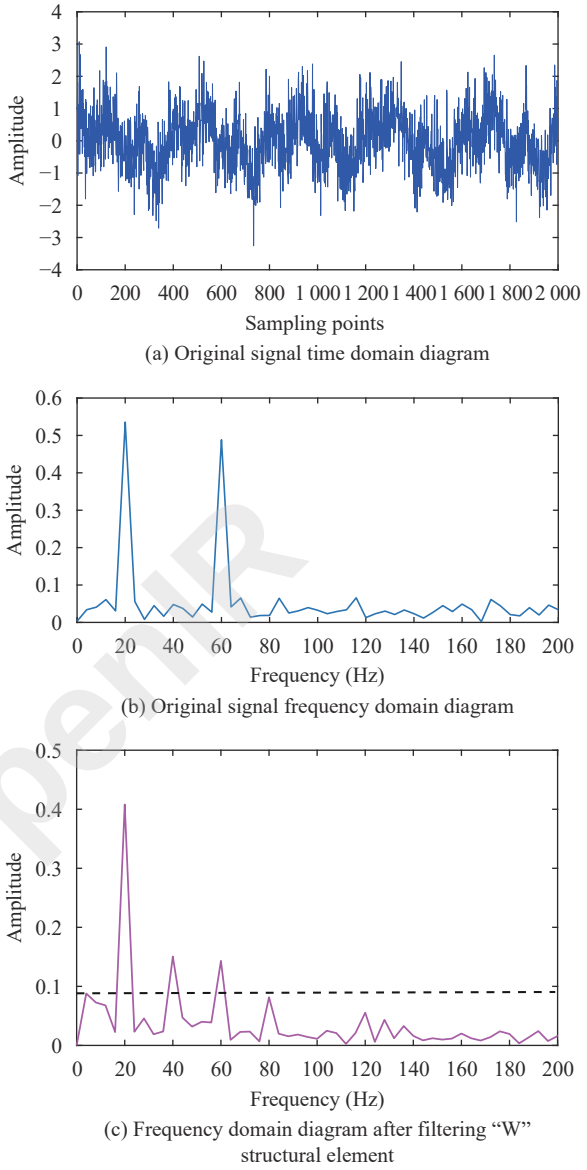

(a) Original signal time domain diagram

(b) Original signal frequency domain diagram

(c) Frequency domain diagram after filtering "W" structural element

Fig. 8 Simulated results of numerical examples

4.3 Case study: Verification of bearing failure data of case western reserve university

In order to further verify the feature extraction effect of the "W" structural elements, this paper uses bearing data from the central experimental platform of Case Western Reserve University to select the vibration signal obtained under a load of 3 HP, speed of 1 730 rpm, and damage diameter of 0.007 mm. The frequency is 12 kHz. The operating conditions of the bearing corresponding to the data include normal, inner ring failure, outer ring failure, and rolling element failure. Outer ring failure has three sampling directions: @3:00, @6:00 and @12:00. Each operating condition contains 25 training sample signals

and 10 test sample signals, and each sample signal contains 2 000 data points, as shown in Table 1.

In order to fully demonstrate the effectiveness of the proposed algorithm, the "W" triangular and flat structural elements are used fault diagnosis, and their diagnostic effects are compared.

Fig. 9 represents the results of fault diagnosis of the inner fault samples of three different structural elements. In Fig. 9, the abscissa shows the signal logarithm, and the ordinate denotes the average correlation coefficient. Figs. 9 (a) and 9 (c) are the fault diagnosis results of the "W" structural element and the flat structural element. The test data have the highest similarity with the inner ring fault, and the target sample is far away from other samples. Hence, it can be accurately judged as an inner ring fault. Fig. 9 (b) displays the fault diagnosis result of the triangular structure element. The test data are very similar to the normal and outer ring fault @6:00 sampling direction specimens. The target standard sample is similar to the normal and outer fault @6:00. The sample distance is relatively close, which is prone to the fault type misjudgment.

Fig. 10 displays the test data samples of rolling element faults utilizing "W" structural elements, triangular structural elements, and flat-shaped structural elements for fault diagnosis results. The fault diagnosis results of "W" structural elements are represented in Fig. 10 (a). The target sample has the highest similarity with the rolling element fault, and the fault type can be determined. However, the target sample is very close to the fault sample in the @12:00 direction of the outer, which is easy to cause misjudgment. Nevertheless, the target sample is mixed with other fault samples in the fault diagnosis results of the triangular structure element and the flat structure element in Figs. 10 (b) and 10 (c). Hence, it is difficult to judge the type of fault. Based on the above analysis, using "W" structural elements to perform multiscale mathematical morphological operations yields a better diagnostic effect on complex faults.

Figs. 11–13 show the fault diagnosis results of the outer ring in the three sampling directions of @3:00, @6:00, and @12:00. As a result of the same fault types, the fault characteristics are also very similar, and the fault types are difficult to distinguish. According to Figs. 11 (a), 12 (a) and 13 (a), the "W" structural elements are used for fault diagnosis. The target sample has the highest similarity with its corresponding fault sample and is far from other fault samples. It can accurately determine the type of fault. Figs. 11 (b), 11 (c), 12 (b), 12 (c), 13 (b) and 13 (c) utilize triangle structure elements and flat structure elements to @3:00 and @6:00 the fault of the outer ring in the two sampling directions of diagnosing. Based on Figs. 11 (b), 11 (c), 12 (b), 12 (c), 13 (b) and 13 (c), the target sample is close to other fault samples, and it is easy to misjudge the fault type.

Table 1 Experimental data of different types of faults

Training samples	Test samples	Damage diameter(mm)	Bearing condition
25	10	0	Normal
25	10	0.007	Inner fault
25	10	0.007	Rolling fault
25	10	0.007	Outer
25	10	0.007	Outer fault
25	10	0.007	Outer fault

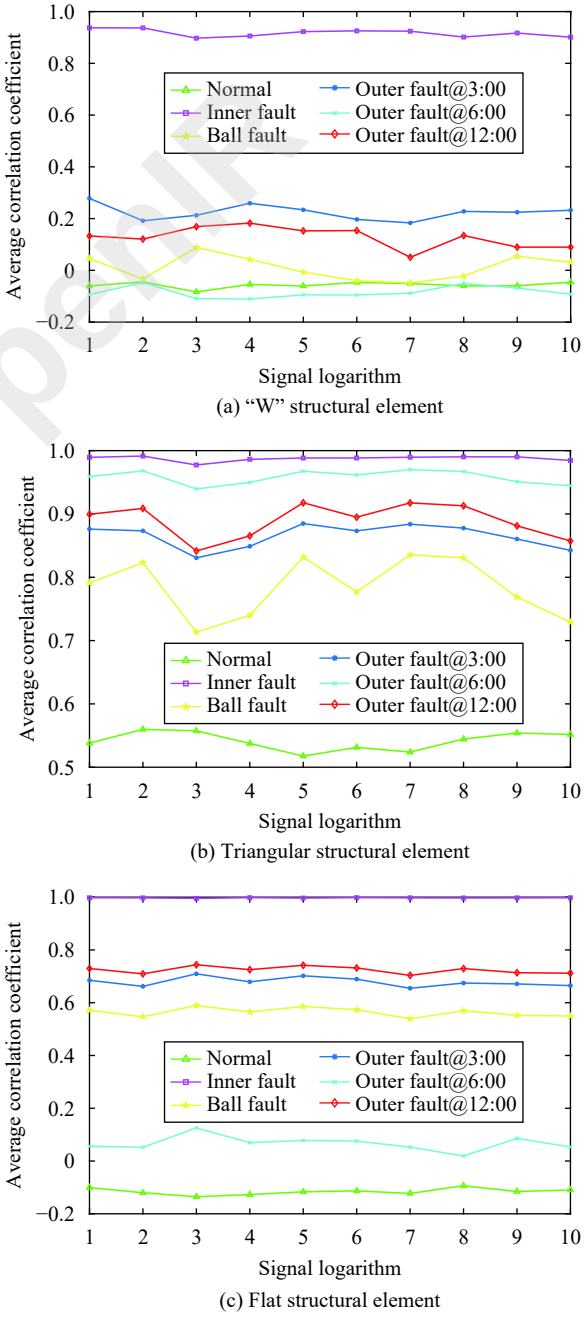

(a) "W" structural element

(b) Triangular structural element

(c) Flat structural element

Fig. 9 Diagnosis results of inner ring fault

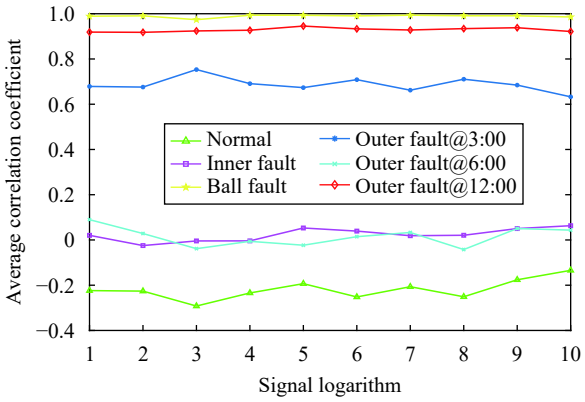

(a) "W" structural element

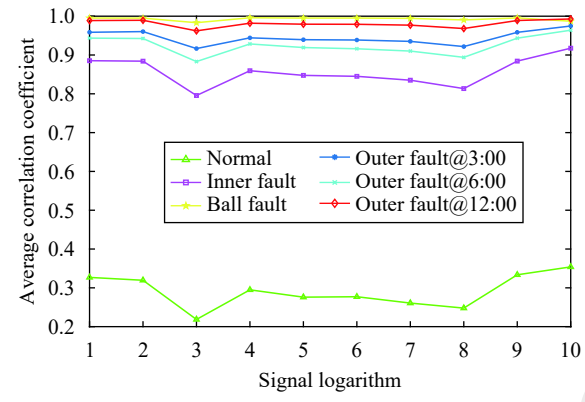

(b) Triangular structural element

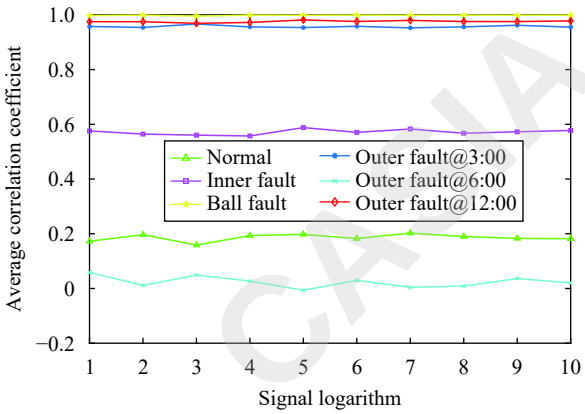

(c) Flat structural element

Fig. 10 Diagnosis result of rolling element fault

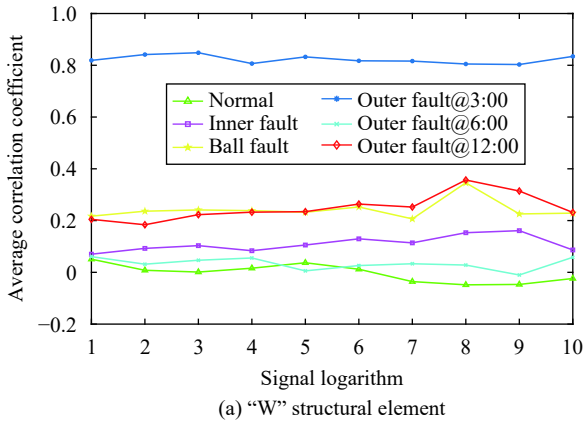

(a) "W" structural element

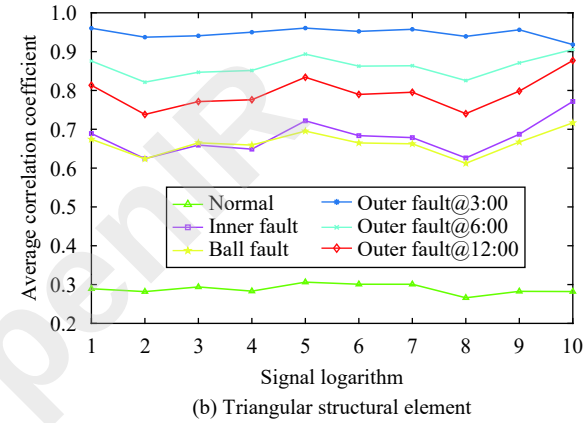

(b) Triangular structural element

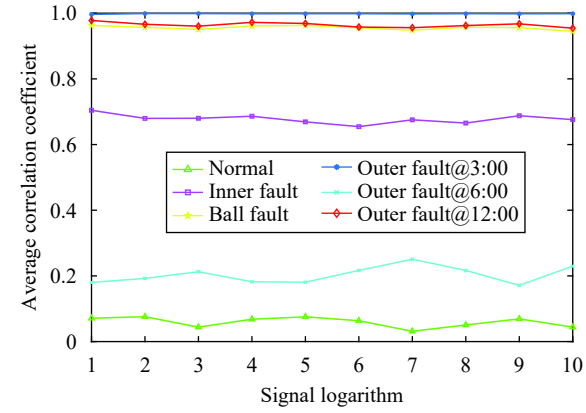

(c) Flat structural element

Fig. 11 Diagnosis result of outer ring fault @3:00

To verify the effectiveness of the adaptive peak energy algorithm, taking the outer fault with the sampling direction @12:00 as an example, the mathematical morphology operation scale is $\lambda = 20$, $\lambda = 50$ and $\lambda = 100$, respectively. The initial structural element is [1 0 1 0 1], and its width increments towards both ends by increasing the scale. Though, its height increases by 0.1 with each scale. Based on the results in Figs. 14 (a) and 14 (b) for fault diagnosis of $\lambda = 20$, $\lambda = 50$ structure, the target samples are closer to the outer fault with the sampling direction @3:00 and rolling element fault which is prone to misjudgment of the type of failures. As a result of the fault diagnosis of λ=100 shown in Fig. 14 (c), the target samples with samples direction to @12:00 of outer fault are the most similar, which can determine the fault type. Although $\lambda = 100$ makes the fault diagnosis effect better, it has a longer running time and lower efficiency. The specific time is shown in Table 2.

According to the time comparison in Table 2, the scale $\lambda = 62$ determined by the adaptive peak energy algorithm results in a fault diagnosis effect similar to $\lambda = 100$. However, the running time is significantly reduced, and the computing efficiency is highly improved.

In order to verify the validity and feasibility of the

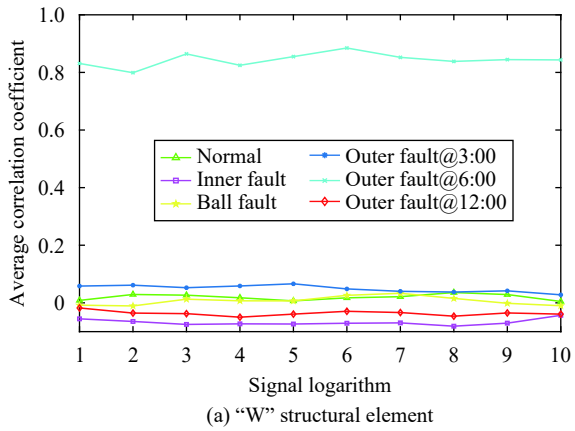

(a) "W" structural element

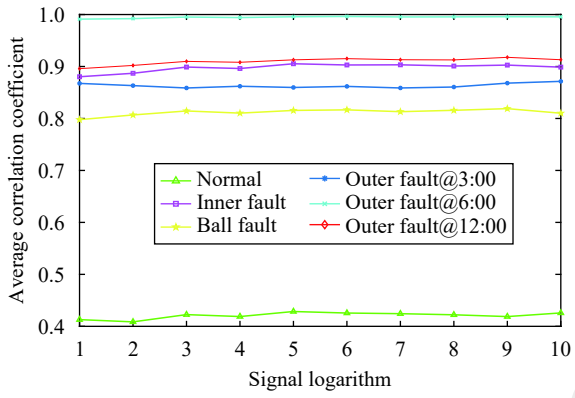

(b) Triangular structural element

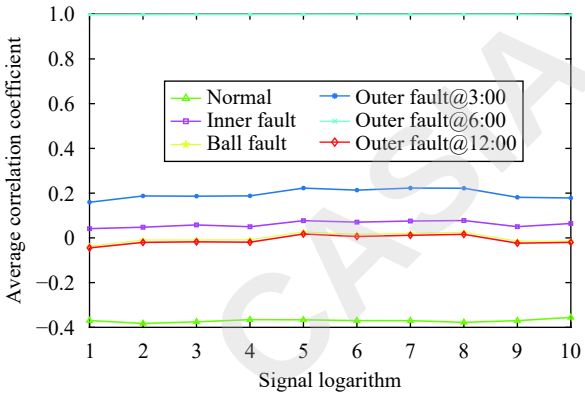

(c) Flat structural element

Fig. 12 Diagnosis result of outer ring fault @6:00

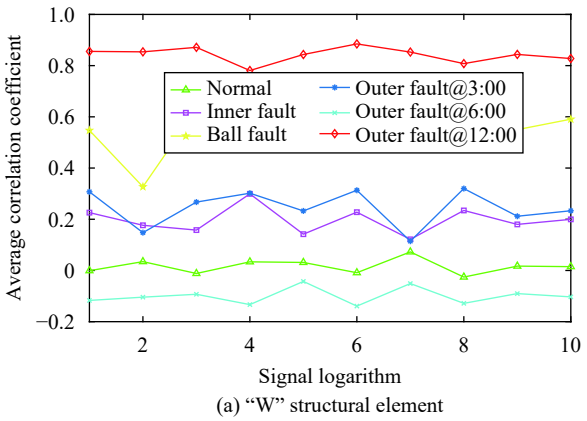

(a) "W" structural element

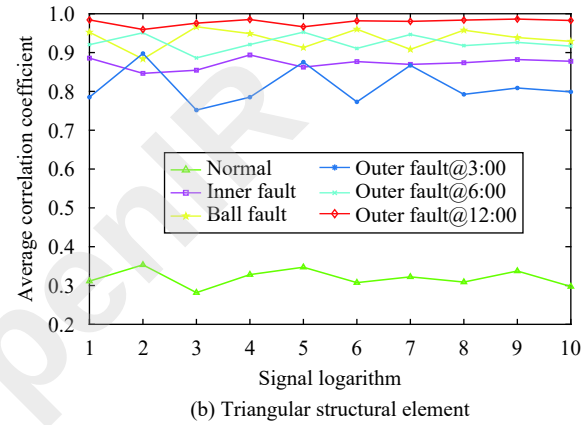

(b) Triangular structural element

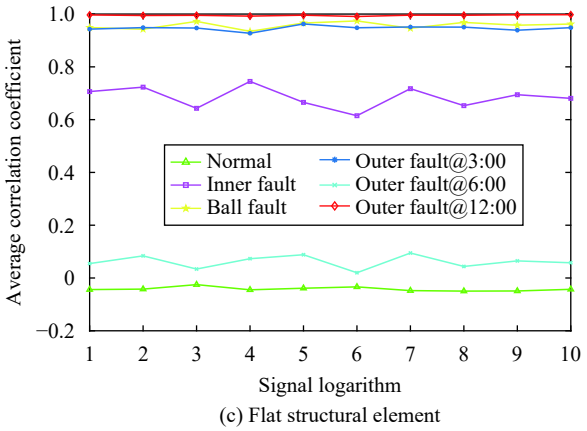

(c) Flat structural element

Fig. 13 Diagnosis result of outer ring fault @12:00

correlation coefficient for fault diagnosis, the inner ring, outer ring, and rolling bearing faults with damage degrees of 0.007 inch, 0.014 inch, and 0.021 inch are selected, and the "W" structural elements are used for fault detection. The results are shown in Fig. 15.

It can be seen in Fig. 15 that the failure of the inner ring, outer ring, and rolling element with a damage degree of 0.007 can be well distinguished from the failures with the other two damage degrees of 0.014 and 0.021. It can be seen that using the method proposed in this article for fault monitoring is capable of not only detecting different types of faults but also predicting the types of faults under different damage signals accurately.

4.4 Application on wind turbines in wind farm

In order to further verify the effect of the proposed algorithm in practical engineering applications, the bearing fault data of wind turbines (model: Yangming 1.5 MW wind turbine) are collected from the Wengongwula wind farm in Inner Mongolia. There are three types of data: outer ring failure, inner ring failure, and normal signal. The sampling frequency is 26 kHz, and the bearing model is 6332MC3SKF deep groove ball bearing. The specific parameters of rolling bearings are shown in Table 3.

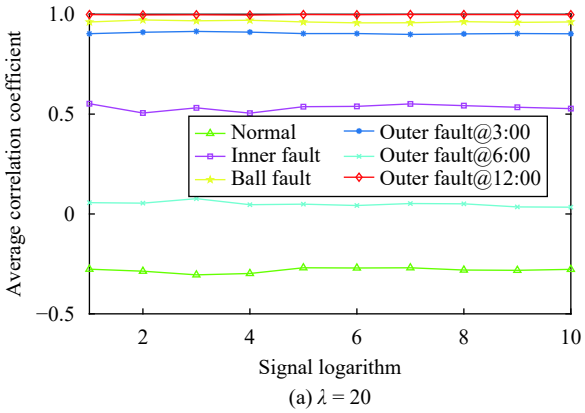

(a) $\lambda = 20$

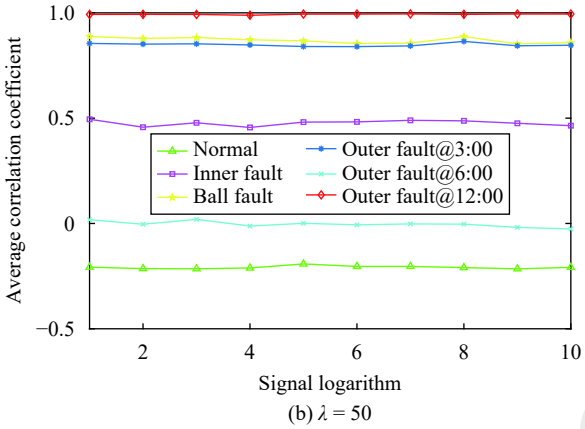

(b) $\lambda = 50$

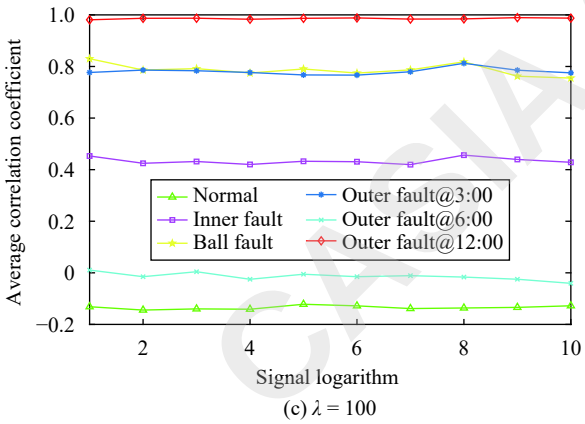

(c) $\lambda = 100$

Fig. 14 Single-scale mathematical morphology fault diagnosis

Table 2 Running time at different scales

Scale		Time (s)
$\lambda = 20$	I7-4720HQ 16.0GB	13.083
$\lambda = 50$		32.923
$\lambda = 100$		153.824
Proposed method $\lambda = 62$		35.558

Each operating condition contains 15 training sample signals and 10 test sample signals. Each training sample signal or test sample signal contains 2 000 data points, which are compared with the extraction effects of triangular and flat structural elements. The diagnosis results of the inner and outer ring faults of the wind turbines are shown in Figs. 16 and 17, respectively. Based on Figs. 16 (a), 16 (b), 17 (a) and 17 (b), "W" shaped structural elements can better diagnose the inner ring and outer ring faults of wind turbine rolling bearings. Moreover, the target sample has the highest similarity with the inner ring fault sample, and the distance from other

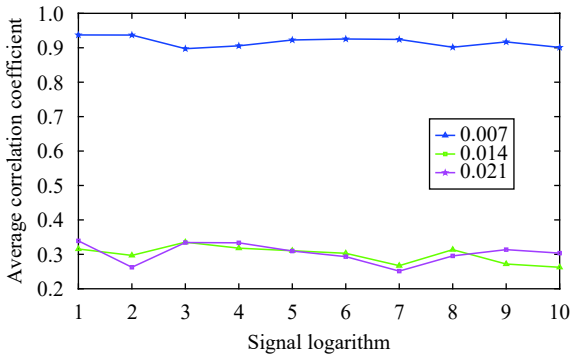

(a) Inner ring failure with damage degree of 0.007, 0.014 and 0.021

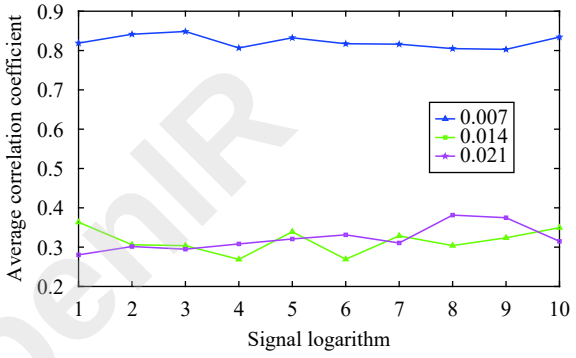

(b) Outer ring failure with damage degree of 0.007, 0.014 and 0.021

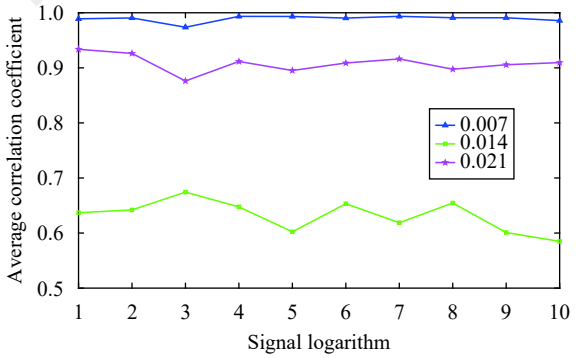

(c) Rolling element failure with damage degree of 0.007, 0.014 and 0.021

Fig. 15 Fault diagnosis results of different damage levels

Table 3 Basic parameters of rolling bearing 6332MC3 SKF

Inner diameter	Outer diameter	Number of rolling elements	Thick-ness	Contact angle
160 mm	340 mm	8	65 mm	0·

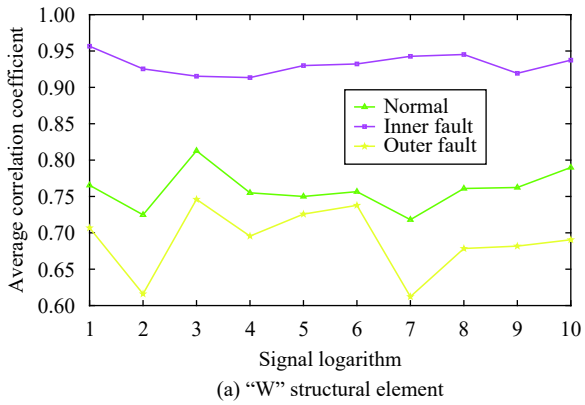

(a) "W" structural element

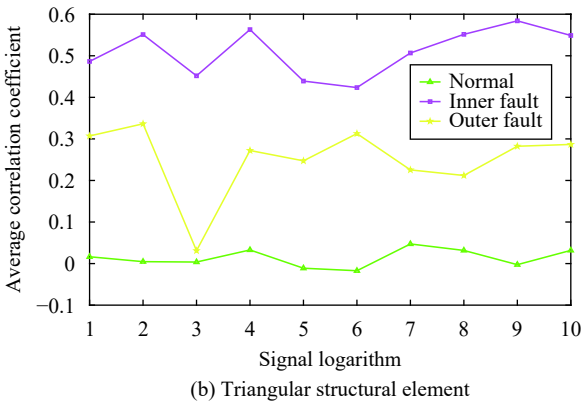

(b) Triangular structural element

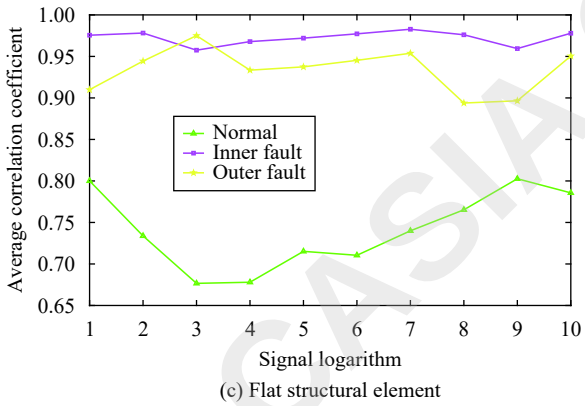

(c) Flat structural element

Fig. 16 Diagnosis result of the inner fault

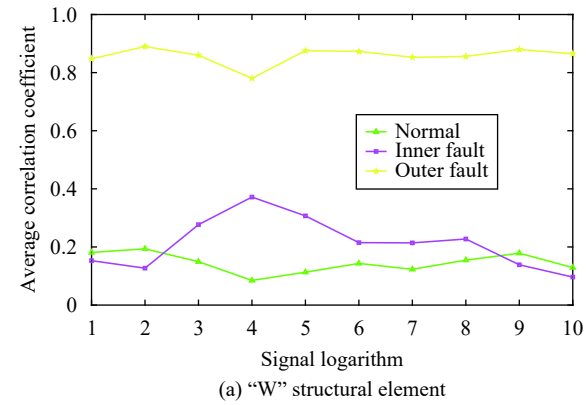

(a) "W" structural element

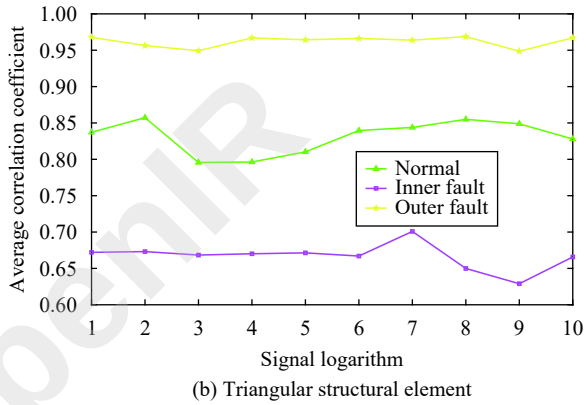

(b) Triangular structural element

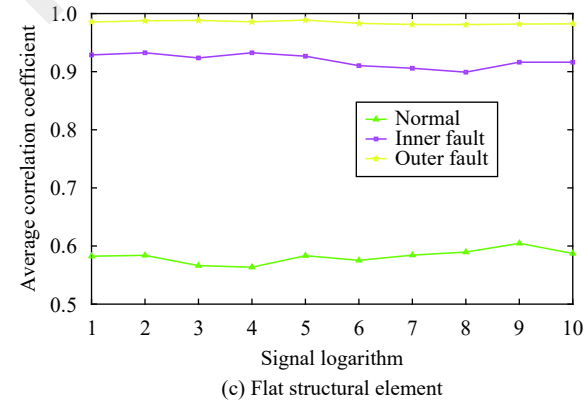

(c) Flat structural element

Fig. 17 Diagnosis result of the outer fault

samples is far. For both the inner and outer ring faults of the triangular structural elements and the flat structural elements, the distance between the target sample and other samples is very close or even mixed. This can easily lead to the misjudgment of the fault type. The effectiveness of the new structural unit in fault feature extraction of an actual wind turbine is further proved.

5 Conclusions

This paper introduces a new type of structural element aiming at the non-linear and non-stationary characteristics of vibration signals of large-scale rolling bearing. It presents the problems of scale selection and multi-scale expansion structure in multi-scale mathematical morphology analysis. The proposed method can effectively overcome the problem of missing the pulse signal in the feature extraction of traditional structural elements. In numerical examples, bearing data of the experimental platform of Case Western Reserve University and real fan data are used to verify the effect of the new structural elements. The obtained results show the effectiveness and practicability of the proposed algorithm.

Acknowledgements

This work was supported by National Natural Science Foundation of China (No. 61763037), Inner Mongolia Autonomous Region Natural Science Foundation of China (No. 2019LH06007), Science and Technology Plan Project

of Inner Mongolia (No. 2019,2020GG028). The authors would like to appreciate the editors and anonymous reviewers for their valuable comments and suggestions.

References

[1] Y. S. Qi, Y. Bai, S. L. Gao, Y. T. Li. Fault diagnosis of wind turbine bearing based on AVMD and spectral correlation analysis. *Acta Energiae Solaris Sinica*, vol. 48, no. 7, pp. 2053–2063, 2019. (in Chinese)

[2] Y. Chai, S. B. Tao, W. B. Mao, K. Zhang, Z. Q. Zhu. Online incipient fault diagnosis based on Kullback-Leibler divergence and recursive principle component analysis. *The Canadian Journal of Chemical Engineering*, vol. 96, no. 2, pp. 426–433, 2018. DOI: 10.1002/cjce.22962.

[3] E. A. Bhuiyan, M. A. Akhand, S. K. Das, F. Ali, Z. Tasneem, R. Islam, D. K. Saha, F. R. Badal, H. Ahamed, S. I. Moyeen. A survey on fault diagnosis and fault tolerant methodologies for permanent magnet synchronous machines. *International Journal of Automation and Computing*, vol. 17, no. 6, pp. 763–787, 2020. DOI: 10.1007/s11633-020-1250-3.

[4] Z. H. Liu, X. D. Meng, H. L. Wei, L. Chen, B. L. Lu, Z. H. Wang, L. Chen. A regularized LSTM method for predicting remaining useful life of rolling bearings. *International Journal of Automation and Computing*, 2021. DOI: 10.1007/s11633-020-1276-6.

[5] J. Serra, L. Vincent. An overview of morphological filtering. *Circuits, Systems and Signal Processing*, vol. 11, no. 1, pp. 47–108, 1992. DOI: 10.1007/BF01189221.

[6] N. G. Nikolaou, I. A. Antoniadis. Application of morphological operators as envelope extractors for impulsive-type periodic signals. *Mechanical Systems and Signal Processing*, vol. 17, no. 6, pp. 1147–1162, 2003. DOI: 10.1006/mssp.2002.1576.

[7] Y. X. Mao, T. X. Su, J. F. Xu, Z. M. Chang. Damage identification method based on axial vibration. *Machine Building & Automation*, vol. 48, no. 3, pp. 137–139, 2019. DOI: 10.19344/j.cnki.issn1671-5276.2019.03.035. (in Chinese)

[8] L. Shen, X. J. Zhou, W. B. Zhang, Z. G. Zhang. De-noising for vibration signals of a rotating machinery based on generalized mathematical morphological filter. *Journal of Vibration and Shock*, vol. 28, no. 9, pp. 70–73, 2009. DOI: 10.3969/j.issn.1000-3835.2009.09.015. (in Chinese)

[9] P. Maragos. Pattern spectrum and multiscale shape representation. *IEEE Transactions on Pattern Analysis and Machine Intelligence*, vol. 11, no. 7, pp. 701–716, 1989. DOI: 10.1109/34.192465.

[10] B. Li, P. L. Zhang, Z. J. Wang, S. S. Mi, D. S. Liu. A weighted multi-scale morphological gradient filter for rolling element bearing fault detection. *ISA Transactions*, vol. 50, no. 4, pp. 599–608, 2011. DOI: 10.1016/j.isatra.2011.06.003.

[11] L. L. Cui, J. L. Wang, J. F. Ma. Early fault detection method for rolling bearing based on multiscale morphological filtering of information-entropy threshold. *Journal of Mechanical Science and Technology*, vol. 33, no. 4, pp. 1513–1522, 2019. DOI: 10.1007/s12206-019-0303-4.

[12] P. B. Zhang. Study on Application of Multi-scale Morphology in Vibration Signal Processing, Master dissertation, North China Electric Power University, China, 2014. (in Chinese)

[13] Z. Wu, S. P. Yang, B. Ren, X. N. Ma, J. C. Zhang. Rolling element bearing fault diagnosis method based on NAMEMD and multi-scale morphology. *Journal of Vibration and Shock*, vol. 35, no. 4, pp. 127–133, 2016. DOI: 10.13465/j.cnki.jvs.2016.04.021.

[14] B. Li, P. L. Zhang, D. S. Liu, S. S. Mi, G. Q. Ren. Feature extraction for roller bearing fault diagnosis based on adaptive multi-scale morphological gradient transformation. *Journal of Vibration and Shock*, vol. 30, no. 10, pp. 104–108, 2011. DOI: 10.3969/j.issn.1000-3835.2011.10.021. (in Chinese)

[15] Y. B. Dong, M. F. Liao, X. L. Zhang, F. Z. Wang. Faults diagnosis of rolling element bearings based on modified morphological method. *Mechanical Systems and Signal Processing*, vol. 25, no. 4, pp. 1276–1286, 2011. DOI: 10.1016/j.ymssp.2010.10.008.

[16] M. Van, P. Franciosa, D. Ceglarek. Rolling element bearing fault diagnosis using integrated nonlocal means denoising with modified morphology filter operators. *Mathematical Problems in Engineering*, vol. 2016, Article number 9657285, 2016. DOI: 10.1155/2016/9657285.

[17] W. Sun, G. A. Yang, Q. Chen, A. Palazoglu, K. Feng. Fault diagnosis of rolling bearing based on wavelet transform and envelope spectrum correlation. *Journal of Vibration and Control*, vol. 19, no. 6, pp. 924–941, 2013. DOI: 10.1177/1077546311435348.

[18] L. J. Zhang, J. W. Xu, J. H. Yang, D. B. Yang, D. D. Wang. Multiscale morphology analysis and its application to fault diagnosis. *Mechanical Systems and Signal Processing*, vol. 22, no. 3, pp. 597–610, 2008. DOI: 10.1016/j.ymssp.2007.09.010.

Qiang Li received the B. Eng. degree in control science and engineering from Inner Mongolia University of Technology, China in 2008. He is a master student of control science and engineering in Inner Mongolia University of Technology, China.

His research interests include condition evaluation, fault monitoring and fault diagnosis of wind power system.

E-mail: 18447070345@163.com
ORCID iD:0000-0002-8505-8556

Yong-Sheng Qi received the B. Eng. degree in control science and engineering from Inner Mongolia University of Technology, China in 1999, and the Ph. D. degree in engineering from University of technology of Beijing, China in 2011. From 2011, he has been working as a professor at Institute of Electric Power, Inner Mongolia University of Technology, China. He is a member of China Artificial Intelligence Association and the reviewers for Chinese journals, including *Control Theory and Application*, *Control Engineering*.

His research interests include fault monitoring and diagnosis for complex industrial processes, condition evaluation, fault monitoring and fault diagnosis of wind power system, and cooperative control technology for mobile robots.

E-mail: qys@imut.edu.cn (Corresponding author)
ORCID iD: 0000-0002-6059-7035

Xue-Jin Gao received the B. Eng. degree in control science and engineering from Hebei University of Science and Technology, China in 1997, and the Ph. D. degrees in engineering from University of technology of Beijing, China in 2006. He has published 2 monographs and more than 50 academic papers, of which more than 50 have been indexed by SCI, EI and

ISTP. He has won the first prize twice and a third prize of provincial science and technology progress, and obtained 15 national invention patents and 3 utility model patents.

His research interests include prediction of key variables in industrial processes, engineering process condition monitoring and fault diagnosis, and biosensor development.

E-mail: gaoxuejin@bjut. edu.cn

Yong-Ting Li received the B. Eng. degree in automation from Taiyuan University of Technology, China in 1998, and the M. Sc. degree in aircraft design from Beijing University of Aeronautics and Astronautics, China in 2005. She has published three software copyrights, and more than 10 papers, including 4 EI indexed papers.

Her research interests include condition assessment, fault monito ring and fault diagnosis of wind turbine system, research on wavelet signal analysis algorithm.

E-mail: liyt@imut.edu.cn

Li-Qiang Liu received the B. Eng. degree in control science and engineering from Inner Mongolia University of Technology, China in 1997, and the Ph. D. degree in electrical engineering from Xi′an Jiaotong University, China in 2010. He has been working as a professor at Center of Electrotechnics Teaching, Inner Mongolia University of Technology, China.

His research interests include circuit theory and its application, substation grounding grid reliability and fault diagnosis.

E-mail: llqiang@imut.edu.cn